

# Dual Aptamer-Functionalized in Situ Injectable Fibrin Hydrogel for Promotion of Angiogenesis via Codelivery of Vascular Endothelial Growth Factor and Platelet-Derived Growth Factor-BB

Nan Zhao,<sup>†</sup> Akiho Suzuki,<sup>†</sup> Xiaolong Zhang,<sup>†</sup> Peng Shi,<sup>†</sup> Lidya Abune,<sup>†</sup> James Coyne,<sup>†</sup> Huizhen Jia,<sup>†</sup> Na Xiong,<sup>‡</sup> Ge Zhang,<sup>§</sup> and Yong Wang<sup>\*,†</sup>

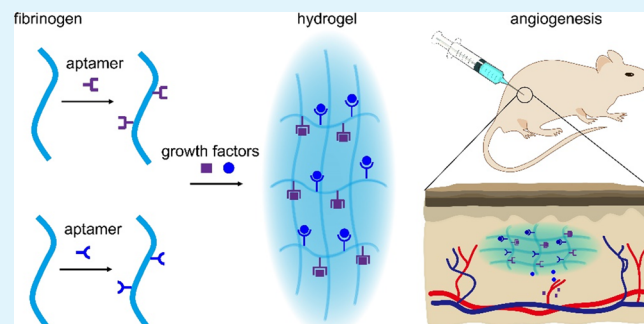
<sup>†</sup>Department of Biomedical Engineering and <sup>‡</sup>Department of Veterinary and Biomedical Sciences, The Pennsylvania State University, University Park, Pennsylvania 16802, United States

<sup>§</sup>Department of Biomedical Engineering, The University of Akron, Akron, Ohio 44325, United States

## Supporting Information

**ABSTRACT:** In situ injectable hydrogels hold great potential for in vivo applications such as drug delivery and regenerative medicine. However, it is challenging to ensure stable sequestration and sustained release of loaded biomolecules in these hydrogels. As aptamers have high binding affinities and specificities against target biomolecules, we studied the capability of aptamers in functionalizing in situ injectable fibrin (Fn) hydrogels for in vivo delivery of two growth factors including vascular endothelial growth factor (VEGF) and platelet-derived growth factor-BB (PDGF-BB). The results show that aptamer-functionalized fibrinogen (Fg) could form in situ injectable Fn hydrogels with porous structures. The aptamer-functionalized Fn hydrogels could sequester more VEGF and PDGF-BB than the native Fn and release these growth factors in a sustained manner with high bioactivity. After the aptamer-functionalized Fn hydrogels were subcutaneously injected into mice, the codelivery of VEGF and PDGF-BB could promote the growth of mature blood vessels. Therefore, this study has successfully demonstrated that aptamer-functionalized in situ injectable hydrogels hold great potential for in vivo codelivery of multiple growth factors and promotion of angiogenesis.

**KEYWORDS:** hydrogel, drug delivery, growth factor, angiogenesis, aptamer



## 1. INTRODUCTION

Hydrogels have been widely studied for in vivo applications such as drug delivery and regenerative medicine.<sup>1–3</sup> Hydrogels are usually preformed before implantation. However, the implantation of hydrogels into target sites requires invasive surgery.<sup>3,4</sup> To minimize the invasiveness of hydrogel implantation, great efforts have been made in developing in situ injectable hydrogels.<sup>5–8</sup> These hydrogels are initially present in the form of solutions before being injected into tissues, having the ability to match any shape or geometry of cavity in target sites. Moreover, delicate biomolecules (e.g., growth factors) can be freshly prepared and dispersed into pregelation solutions right before in vivo delivery, which ensures the maintenance of their bioactivity that may be easily lost during the long-term storage in a preformed hydrogel.

In principle, polymer solutions that are sensitive to the variation of temperature, ions, enzymes, pH, and light can be used to develop in situ injectable hydrogels.<sup>9–11</sup> For instance, the copolymer of polyethylene glycol and poly( $\epsilon$ -caprolactone) can form a hydrogel with the variation of the temperature,<sup>12</sup> alginate can form an ionic hydrogel in the presence of divalent ions,<sup>13</sup> and fibrinogen (Fg) can form a fibrin (Fn) hydrogel in

the presence of thrombin.<sup>14</sup> However, like most preformed hydrogels, in situ injectable hydrogels are highly permeable.<sup>3</sup> The high permeability will lead to the rapid release of loaded cargos.<sup>15</sup> As injectable hydrogels are mainly used for drug delivery and regenerative medicine applications, it is important to functionalize them to ensure stable sequestration and sustained release of loaded cargos.

Aptamers hold great potential for the functionalization of injectable hydrogels in sequestering loaded cargos. Aptamers are single-stranded oligonucleotides selected from synthetic RNA/DNA libraries. They bind to target molecules with high affinities and specificities.<sup>16,17</sup> Moreover, as they are usually short with 20 to 60 nucleotides, they can be synthesized and modified with standard methods of chemical synthesis and conjugation. Several aptamers have been approved for clinical applications.<sup>17</sup> For example, pegaptanib, which is a vascular endothelial growth factor (VEGF)-binding RNA aptamer, has been used in treating age-related macular degeneration.<sup>18</sup> Our

**Received:** February 7, 2019

**Accepted:** April 26, 2019

**Published:** April 26, 2019

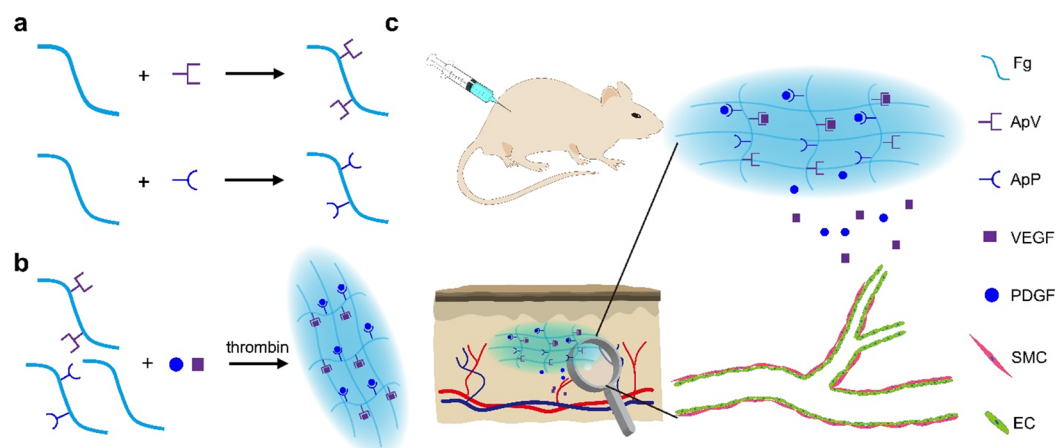


**Figure 1.** Schematic illustration of dual aptamer-functionalized Fn hydrogels for codelivery of angiogenic factors and promotion of angiogenesis. (a) Functionalization of Fg with ApV or ApP. (b) Synthesis of Fn-Ap hydrogels loaded with growth factors. (c) Stimulation of angiogenesis using Fn-Ap hydrogels loaded with VEGF and PDGF-BB. Fg, native fibrinogen; VEGF, vascular endothelial growth factor; PDGF, platelet-derived growth factor-BB; ApV, anti-VEGF aptamer; ApP, anti-PDGF-BB aptamer; SMC, smooth muscle cell; EC, endothelial cell.

group has pioneered the development of aptamer-functionalized hydrogel systems for protein sequestration and sustained release,<sup>19–25</sup> which has also been confirmed by many others.<sup>26–28</sup> However, most of these previous studies were performed *in vitro*. In particular, no direct evidence has been provided to show the effectiveness of aptamers in functionalizing *in situ* injectable hydrogels for *in vivo* applications, and no study has been performed to examine aptamer-mediated *in vivo* delivery of multiple cargos.

Fn is an FDA-approved material for hemostats, sealants, and adhesives.<sup>29</sup> Fn and Fn-based hydrogel have been extensively used in clinical and preclinical applications such as wound dressings and drug delivery systems.<sup>30</sup> Soluble Fg molecules can be cured *in situ* to form injectable and biodegradable Fn hydrogels.<sup>31</sup> Moreover, Fn hydrogels form under physiological conditions that benefit the maintenance of high bioactivity of loaded cargos. Thus, the purpose of this study was to use Fn as a model to examine whether two different aptamers can be used to functionalize *in situ* injectable hydrogels for *in vivo* delivery of dual growth factors and promotion of angiogenesis (Figure 1). The two aptamers used herein bind VEGF and platelet-derived growth factor-BB (PDGF-BB). We performed *in vitro* studies to examine aptamer-mediated VEGF and PDGF-BB release and also injected aptamer-functionalized Fn (Fn-Ap) hydrogels subcutaneously into mice to evaluate the effect of VEGF and PDGF-BB codelivery on the promotion of angiogenesis.

## 2. MATERIALS AND METHODS

**2.1. Materials.** **2.1.1. Chemical Reagents.** Sodium bicarbonate (NaHCO<sub>3</sub>), calcium chloride (CaCl<sub>2</sub>), acrylic acid *N*-hydroxysuccinimide ester (AA-NHS), tris(2-carboxy ethyl) phosphine hydrochloride (TCEP), dimethyl sulfoxide (DMSO), Tween-20, and Cytodex 3 microcarrier beads were purchased from Sigma-Aldrich (St. Louis, MO). Tris-HCl buffer, sodium dodecyl sulfate, Trizma base, sodium chloride, hydrogen chloride, reagent alcohol, glycerol, acrylamide/bis(acrylamide), tris-borate-EDTA (TBE) buffer, phosphate-buffered saline (PBS), and Dulbecco's phosphate-buffered saline (DPBS) were obtained from Thermo-Fisher Scientific (Waltham, MA).

**2.1.2. Biological Reagents.** Thrombin, benzoyl-DNAse (DNase), and bicinchoninic acid (BCA) protein assay kit were obtained from Sigma-Aldrich. Calcein AM, Live/Dead Cell Viability Assay, glycine, bovine serum albumin (BSA), fetal bovine serum

(FBS), trypsin-EDTA, Medium 200 (M200), Medium 231 (M231), Low Serum Growth Supplement kit (LSGS), Xylene Substitute Mountant, ProLong Diamond Antifade Mountant with DAPI, goat anti-rabbit IgG-Alexa Fluor 546 antibody, and  $\alpha$ -smooth muscle actin antibody-Alexa Fluor 488 antibody ( $\alpha$ -SMA) were obtained from Thermo-Fisher Scientific. Nucleic acid sequences (Table S1) were obtained from Integrated DNA Technologies (Coralville, IA). Paraformaldehyde solution (4%) and human Fg were obtained from Millipore (Billerica, MA). Vascular endothelial growth factor-165 (VEGF), platelet-derived growth factor-BB (PDGF-BB), VEGF enzyme-linked immunosorbent assay (ELISA) kit, and PDGF-BB ELISA kit were obtained from PeproTech (Rocky Hill, NJ). Primary rabbit anti-mouse CD31 was obtained from Cell Signaling Technology (Beverly, MA). Hematoxylin and eosin (H&E) stain kit was obtained from Leica Biosystems (Buffalo Grove, IL). Human umbilical vein endothelial cells (HUVECs) were obtained from Thermo-Fisher Scientific. Human aorta smooth muscle cells (HASMCs) were obtained from ATCC (Manassas, VA).

**2.2. Methods.** **2.2.1. Functionalization of Fg with Aptamers.** Fg was functionalized with anti-VEGF aptamers (ApV) or anti-PDGF-BB aptamers (ApP), as previously reported.<sup>32</sup> Briefly, native Fg was reacted with NHS-acrylate in NaHCO<sub>3</sub> buffer (pH = 8) for 4 h. Byproducts were removed by washing the reaction mixture in a 100 kDa filter. Thiolate anti-VEGF aptamers or thiolate anti-PDGF-BB aptamers were reduced in 50 mM TCEP at room temperature for 1 h. The reduced aptamers were mixed with the acrylate-Fg in tris-HCl buffer, and the reaction was carried out at 37 °C for 4 h. Unreacted aptamers and byproducts were removed by filtering the mixture with a 100 kDa molecular filter. The amount of free aptamers in the eluent was quantified by a nanodrop and used to calculate the conjugation efficiency. Fg functionalized with anti-VEGF aptamers and anti-PDGF-BB aptamers was denoted as Fg-V and Fg-P, respectively. Fg functionalized with aptamers was denoted as Fg-Ap (including Fg-V and Fg-P).

**2.2.2. Gel Electrophoresis.** Two microliters of the diluted Fg-V or Fg-P was incubated with 50 pmol of their corresponding complementary DNA sequence (cDNA) labeled with fluorescent molecules at 37 °C for 1 h. Then, the mixtures were loaded to polyacrylamide gel and run at 80 V for 45 min. The gel was imaged with a Maestro imaging system (CRI, Woburn, MA). The cDNA of ApV was labeled with fluorescein amidite (FAM), and the cDNA of ApP was labeled with cyanine 5 (Cy5).

**2.2.3. Turbidity Assay.** The turbidity assay was performed according to a published paper.<sup>33</sup> Equal amount of Fg-V and Fg-P was combined. Native Fg was supplemented with varying amounts of Fg-V and Fg-P to make the final Fg-Ap 0, 20, 40, 60, and 100% of the total Fg. The final total concentration of Fg was 8 mg/mL. Then, 50

$\mu\text{L}$  of the total solution was added to a 96-well plate. After the addition of a 50  $\mu\text{L}$  mixture of 0.4 U/mL thrombin and 20 mM  $\text{CaCl}_2$ , the turbidity of the solution was monitored with an Infinite M200 Pro microplate reader (Tecan, Grödig, Austria).

**2.2.4. Bulk Hydrogel Imaging.** Native Fg was supplemented with equal volume of Fg-V and Fg-P to make the final native Fg 50% of the total Fg in a glass vial (10 mg/mL of total Fg). Then,  $\text{CaCl}_2$  and thrombin were added to the glass vial to make the final total concentrations of thrombin (1 U/mL) and  $\text{CaCl}_2$  (10 mM). Images of the solution in the glass vial were taken at 0 and 10 min after adding the thrombin and  $\text{CaCl}_2$  solution.

**2.2.5. Hydrogel Synthesis.** For all the hydrogels used thereafter, the final total concentration of Fn was 10 mg/mL, and the concentration of thrombin was 1 U/mL. To synthesize the aptamer-functionalized Fn hydrogels, Fg was mixed with different amount of Fg-V or/and Fg-P. Then, equal volume mixture of thrombin and  $\text{CaCl}_2$  was added to the Fg mixture. Fn hydrogels functionalized with anti-VEGF aptamers and Fn hydrogels functionalized with anti-PDGF-BB aptamers were denoted as Fn-V and Fn-P, respectively. Fn hydrogels functionalized with both aptamers were denoted as Fn-B. Fn hydrogels functionalized with aptamers were denoted as Fn-Ap (including Fn-V, Fn-P, and Fn-B). To prepare growth factor-loaded hydrogels, VEGF or/and PDGF-BB were mixed with the Fg-Ap before adding the thrombin and  $\text{CaCl}_2$  mixture.

**2.2.6. Aptamer Imaging.** Disk Fn and Fn-B hydrogels (4  $\mu\text{M}$  aptamers) were stained with fluorescent-labeled complementary DNA (cDNA) of the aptamers, washed with PBS, and imaged with a Maestro Imaging System (CRI, Woburn, MA). For confocal imaging, the hydrogels were fixed in 4% paraformaldehyde, stained, washed, and imaged with a confocal microscope (Olympus FV1000, Center Valley, PA).

**2.2.7. Scanning Electron Microscopy.** Fn and Fn-B hydrogels (4  $\mu\text{M}$  aptamers) were fixed in 4% paraformaldehyde solution and lyophilized in a freeze dryer (Labconco, Kansas City, MO). Then, the lyophilized samples were sputter-coated and imaged with a field-emission SEM (Zeiss Sigma, US).

**2.2.8. Growth Factor Retention and Release.** Fn-V (0, 0.06, 0.12, 0.24, 0.48, and 0.96  $\mu\text{M}$  ApV) loaded with 50 ng of VEGF or Fn-P (0, 0.1, 0.2, 0.4, 0.8, and 1.6  $\mu\text{M}$  ApP) loaded with 50 ng of PDGF-BB was synthesized. Growth factor-loaded hydrogels were incubated with 1 mL of release media (DPBS supplemented with 0.1% BSA or basal cell culture media supplemented with 0.1% BSA). After 24 h, the release media were collected and stored at  $-20\text{ }^\circ\text{C}$ . For the experiments of sustained VEGF release, mole ratios of 20:1 (ApV/VEGF) and 10:1 (ApP/PDGF-BB) were used. Two hundred nanograms of VEGF and/or 200 ng of PDGF-BB was loaded to different hydrogels. Hydrogels were incubated with 1 mL of release medium. The release media were collected and replenished with 1 mL of fresh release media at different day. For Fn-B hydrogels loaded with both VEGF and PDGF-BB, the aptamers in the hydrogel were lysed with 100 U/mL DNase at day 14 to retrieve the remaining growth factor in the hydrogel. The concentration of growth factor in the release media was analyzed using ELISA kits according to the protocol provided by the manufacturer.

**2.2.9. Cell Culture.** HUVECs were expanded in M200 supplemented with 2% LSGS, and HASMCs were expanded in M231 supplemented with 10% FBS. HUVECs and HASMCs of passages 4 to 10 were used in all cell experiments.

**2.2.10. Cell Survival Assay.** Confluent HUVECs were starved in M200 supplemented with 1% FBS overnight. The released media from day 14 were diluted using basal cell culture media to make the final concentration of growth factor around 10 ng/mL and supplemented with 1% FBS. Then, cells were treated with M200 supplemented with 1% FBS, the diluted VEGF release media from Fn-V, or the diluted VEGF release media from Fn-B. After 2 days, the remaining HUVECs were stained with Live/Dead Cell Viability Assay and imaged with an Olympus IX73 microscope (Center Valley, PA).

**2.2.11. Cell Migration Assay.** Cell migration was evaluated through Boyden chamber assay. HUVECs ( $2 \times 10^4$ ) or HASMCs ( $2 \times 10^4$ ) were seeded into the insert of a 24-well Transwell plate (8  $\mu\text{m}$  pore)

and immersed in complete culture medium for 6 h to allow cell attachment. Then, the complete media were changed into 1% FBS-supplemented basal media. Six hundred microliters of different diluted release media from day 14 was added to the bottom of the Transwell. After 12 h, cells on the upper side of the membrane were removed using a cotton swab. Cells that migrated down to the membrane were stained with Calcein AM and imaged with the Olympus IX73 microscope. The number of migrated cells was quantified in ImageJ.

**2.2.12. Cell Proliferation Assay.** HUVECs ( $4 \times 10^4$ ) or HASMCs ( $4 \times 10^4$ ) were seeded into each well of a 24-well cell culture plate. Cells were starved in 1% FBS-supplemented basal media for 12 h. Then, the media were changed into different diluted release media from day 14 or basal media supplemented with 1% FBS. At predetermined days (day 7 for HUVECs and day 5 for HASMCs), cells were imaged with a microscope, and cell numbers were quantified in ImageJ. The number of cells at the end of the experiment was normalized to the initial number of cells.

**2.2.13. Microbeads Assay.** Cytodex 3 microcarrier beads were diluted into PBS and autoclaved. HUVECs were seeded to the beads at a density of 50 cells per bead. The beads coated with cells were embedded into native Fn loaded with 50 ng of VEGF and 50 ng of PDGF-BB (Fn + VP), Fn-V loaded with 50 ng of VEGF, Fn-P loaded with 50 ng of PDGF-BB, or Fn-B loaded with 50 ng of VEGF and 50 ng of PDGF-BB. After adding the M200 supplemented with 2% FBS, cells were cultured for 5 days. Cell culture media were changed every day. At day 5, cells in the beads were stained with Calcein AM and imaged. The number of sprouting branches of endothelial cells was quantified in ImageJ. The branches were only counted when the sprouting endothelial cells were attached to the beads and the length of the sprouting endothelial cells was longer than half of the diameter of the bead.

**2.2.14. Aorta Ring Assay.** Aorta ring assay was performed as described by a previously published protocol.<sup>34</sup> Briefly, the thoracic aorta of BALB/c mice was collected and cut into rings with a length of 0.5 mm. The rings were starved in DMEM supplemented with 1% FBS overnight. After the rings were embedded in 50  $\mu\text{L}$  of collagen gel (1.5 mg/mL), native Fn loaded with 100 ng of VEGF and 100 ng of PDGF-BB (Fn + VP), Fn-V loaded with 100 ng of VEGF, Fn-P loaded with 100 ng of PDGF-BB, or Fn-B loaded with 100 ng of VEGF and 100 ng of PDGF-BB was added to the top of the collagen hydrogels. One hundred microliters of DMEM supplemented with 2% FBS was added to each ring. At day 5, the rings were stained with Calcein AM and imaged. The lengths of three longest sprouts in each image were quantified and averaged. The area of sprouts was normalized to the diameter of the aorta. Only the sprouts connected to the aorta were quantified.

**2.2.15. In Vivo Angiogenesis.** A mouse subcutaneous injection model was performed according to the protocol approved by the Pennsylvania State University Institutional Animal Care and Use Committee (IACUC). Female BALB/c mice (age of 7 weeks) were used. The dorsal hair of the mice was removed using an electronic razor followed by Veet depilatory cream treatment. One hundred twenty microliters of native Fn loaded with 200 ng of VEGF and 200 ng of PDGF-BB, Fn-V hydrogel loaded with 200 ng of VEGF, Fn-P loaded with 200 ng of PDGF-BB, and Fn-B loaded with 200 ng of VEGF and 200 ng of PDGF-BB was subcutaneously injected to the dorsal flanks of the mice with a 27-gauge needle. Two hydrogels were injected into each mouse. The positions of the injected hydrogels were visible to the naked eye for around 14 days post-implantation. To track the location of the hydrogels after 14 days, the position of hydrogels was labeled with a black marker starting at day 12 post-implantation. After 5, 10, or 20 days, mice were sacrificed with  $\text{CO}_2$  asphyxiation, and tissues around the hydrogel were collected. The tissues were fixed in 4% paraformaldehyde solution, embedded in paraffin, and used for further staining.

**2.2.16. H&E Staining.** Paraffin-embedded tissue samples were sectioned into slices of 5  $\mu\text{m}$  and stained with H&E stain kit using a Leica Autostainer (Buffalo Grove, IL). Then, the stained tissue slides were mounted using Xylene Substitute Mountant and allowed to dry

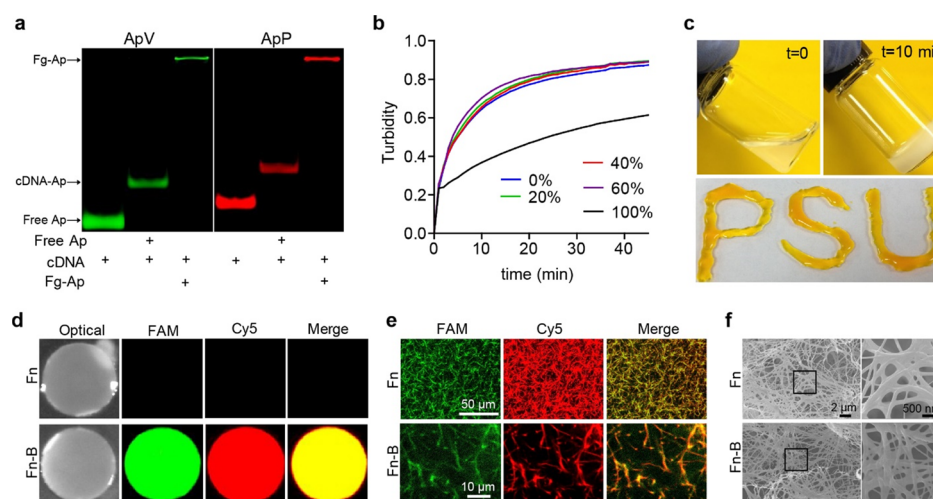


**Figure 2.** Synthesis and characterization of aptamer-functionalized Fn (Fn-Ap) hydrogels. (a) Gel electrophoresis of Fg-Ap stained with fluorophore-labeled complementary DNA sequence (cDNA). ApV, anti-VEGF aptamer; ApP, anti-PDGF-BB aptamer; Ap, aptamer; cDNA-Ap, cDNA-Ap complex. cDNA of ApV was labeled with fluorescein amidite (FAM), and cDNA of ApP was labeled with cyanine 5 (Cy5). (b) Effect of Fg-Ap concentration on self-assembly. Fg-V and Fg-P had the same concentration in the Fg-Ap solution. (c) Optical images of dual aptamer-functionalized Fn hydrogels (Fn-B). Upper panel: States of Fn-B before and after gelation. Lower panel: Extrusion of Fn-B from a 27-gauge needle. Fn-B was mixed with dye for clear legibility. (d) Fluorescence images of whole hydrogels. Hydrogels were stained with fluorophore-labeled cDNAs. (e) Confocal images showing networks and fibers of Fn-B. (f) Scanning electron microscopy images.

at room temperature. The images were taken with a BZ-X700 microscope (Keyence, Itasca, IL).

**2.2.17. Immunostaining.** Paraffin-embedded tissue samples were sectioned into slices of 5 μm and deparaffinized. The deparaffinized samples were boiled in sodium citrate buffer (pH = 6) for 20 min. After the sections were blocked with serum blocking solution (3% of BSA and 3% of goat serum in PBS) for 1 h at room temperature, the samples were incubated with rabbit anti-mouse CD31 antibody (1:200 dilution) overnight at 4 °C. Then, the samples were washed with PBS and incubated with goat anti-rabbit IgG-Alexa Fluor 546 secondary antibody (1:200 dilution) for 2 h at room temperature. The tissues were incubated with fluorescent-labeled α-SMA antibody (1:200 dilution) overnight at 4 °C. After washing with PBS, the samples were mounted using ProLong Diamond Antifade Mountant with DAPI. The fluorescence images of the sample were taken with the Olympus IX73 microscope, and the total number of blood vessels per field was quantified with ImageJ. Individual cells without a lumen structure were excluded from the count. All the vessels with CD31 signal were defined as CD31<sup>+</sup> blood vessels. The blood vessels with both CD31 signal and α-SMA signal were defined as α-SMA<sup>+</sup> blood vessels.

**2.2.18. Statistics.** Prism 5.0 (GraphPad Software Inc., La Jolla) was used for all the statistical analysis. All the data were presented as mean ± standard deviation, unless otherwise specified. One-way analysis of variance (ANOVA) with the Bonferroni post-test was performed to compare multiple groups. The data were considered statistically different when  $p < 0.05$ .

### 3. RESULTS AND DISCUSSIONS

**3.1. Synthesis and Characterization of Dual Aptamer-Functionalized Fn Hydrogels.** Hydrogels have been extensively studied to develop growth factor delivery systems for therapeutic angiogenesis because of their biophysical and biochemical similarity to native tissues.<sup>35–37</sup> One major drawback of hydrogels for growth factor delivery is the quick release of loaded growth factors due to the high permeability of hydrogels.<sup>3</sup> The fast release of angiogenic growth factors from the hydrogel can not only lead to short therapeutic duration but also cause toxic side effects.<sup>38,39</sup> In addition, multiple growth factors are needed at different stages during the process

of angiogenesis.<sup>40</sup> For instance, VEGF is important for initiating the angiogenesis process, and PDGF-BB is important for stabilizing newly formed blood vessels.<sup>41</sup> Thus, a functional hydrogel delivery system may need to release a high amount of some angiogenic factors such as VEGF at an earlier stage and release others such as PDGF-BB more slowly in a sustained manner to enable the formation of mature vessels. Fn hydrogels have been studied with the ability to prolong the release of VEGF.<sup>32</sup> It has also been reported that sustained VEGF release could promote better angiogenesis compared with bolus delivery.<sup>42,43</sup> However, VEGF alone may not be enough to promote the formation of mature and stable blood vessels.<sup>44</sup> Thus, to facilitate mature and stable blood vessel formation, we incorporated both anti-VEGF and anti-PDGF-BB aptamers into the Fn system.

We first functionalized Fg with the acrylate group and then conjugated Fg and aptamers via thiol-ene reaction. We used this method because native Fg has around 200 primary amine groups that are adequate for reaction with NHS-acrylate for aptamer conjugation. Compared with previously reported methods using the cysteine groups for polyethylene glycol (PEG) conjugation,<sup>45</sup> this method is independent of the reduction of the disulfide bonds of Fg and is less likely to change the structure of Fg. Thus, Fg-Ap would form a hydrogel under the catalysis of thrombin.

Our data show that ApV and ApP could be successfully conjugated with Fg (Figure 2a). The conjugation efficiency of ApV and ApP to Fg was 34.5 and 32.7%, respectively (Table S2). After the conjugation, we examined whether aptamer functionalization affected the Fg assembly process. We mixed native Fg with different amounts of Fg-Ap (equal amounts of Fg-V and Fg-P). The dynamic assembly curves show that pure Fg-Ap could undergo self-assembly, while the assembly kinetics was slowed (Figure 2b). This slowed assembly may be attributed to steric hindrance caused by aptamers in Fg-Ap. However, when the initial percentage of Fg-Ap was 60% or lower, aptamer functionalization barely affected the thrombin-catalyzed Fn assembly process (Figure 2b). To examine

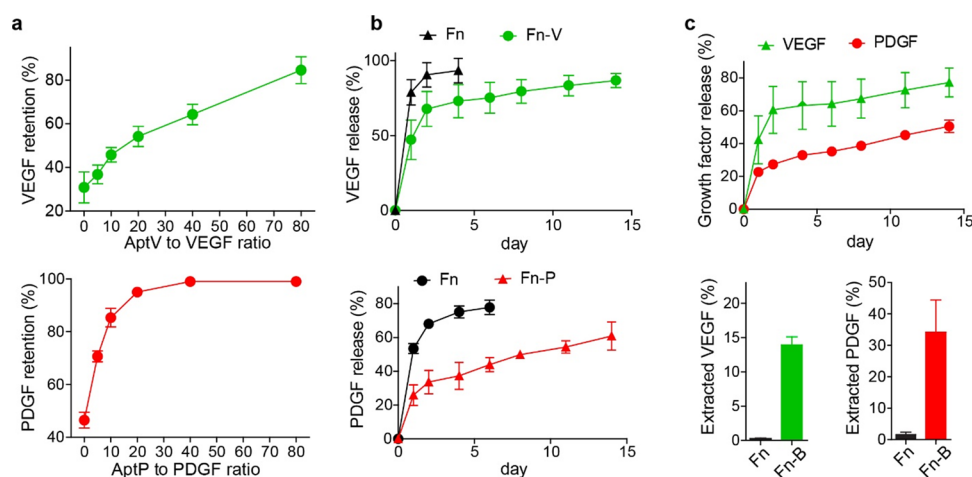


**Figure 3.** Retention and release of VEGF and PDGF-BB. (a) Growth factor retention. Upper panel: VEGF retention in ApV-functionalized hydrogels (Fn-V); lower panel: PDGF-BB retention in ApP-functionalized hydrogels (Fn-P). (b) Aptamer-mediated individual release of VEGF or PDGF-BB. The ApV-to-VEGF ratio was 20:1. The ApP-to-PDGF-BB ratio was 10:1. (c) Dual aptamer-mediated release of VEGF and PDGF-BB from the Fn-B hydrogels. Bottom figures show the amounts of VEGF and PDGF-BB extracted from the Fn-B hydrogels at day 14 ( $n = 3$ ).

whether Fg-Ap can form in situ injectable hydrogels, native Fg was supplemented with an equal amount of Fg-V and Fg-P. The images show that the reaction mixture formed a bulk hydrogel stably attached to the bottom of the vial (Figure 2c). We also loaded the reaction mixture into a 27-gauge syringe. The reaction mixture could be extruded to form a stable hydrogel (Figure 2c), which suggests that it is feasible to perform in vivo delivery of the pre-gel solution using a syringe.

We further stained the hydrogels to confirm the incorporation of aptamers into the hydrogels. ApV was stained with its FAM-labeled cDNA, and ApP was stained with its Cy5-labeled cDNA. No fluorescence signal was detectable in the native Fn hydrogel (Figure 2d). Fn-V exhibited only green fluorescence signal and Fn-P exhibited only red fluorescence signal (Figure S1a). Fn-B exhibited both green and red signals (Figure 2d). It suggests that both Fg-V and Fg-P were incorporated into the Fn-B hydrogel. We then examined the fibers of Fn-B with confocal microscopy. Each fiber of Fn-B exhibited both green and red fluorescence signals (Figure 2e). We also imaged the lyophilized hydrogels with SEM. Fn-B, native Fn, Fn-V, and Fn-P all formed similar structures (Figure 2f and Figure S1b), which confirms that aptamer incorporation did not change the overall microstructure of Fn hydrogel.

**3.2. In Vitro Release of Growth Factors.** Aptamers can bind to their target molecules with high affinities and high specificities. The presence of aptamers in hydrogels would increase the retention of target biomolecules via affinity binding. Moreover, the release of loaded biomolecules would be governed by both diffusion and affinity binding. To test whether the Fn-Ap can retain growth factors, we first loaded VEGF to Fn-V and PDGF-BB to Fn-P. VEGF retention in Fn-V virtually linearly increased with the increasing ApV-to-VEGF ratio (Figure 3a). In comparison, native Fn could retain more PDGF-BB than VEGF, which may be attributed to stronger nonspecific fibrin–PDGF-BB interactions.<sup>46</sup> Notably, PDGF-BB retention increased logarithmically with the increased ratio of ApP to PDGF-BB. When the ratio of ApP to PDGF-BB was over 20, PDGF-BB retention was more than 95%.

We next examined the sustained release of VEGF and PDGF-BB. Over 90% of the loaded VEGF was released from the native Fn within 3 days. By contrast, in the presence of

ApV, VEGF release from Fn-V hydrogels was significantly slowed down (Figure 3b). Similar to ApV-mediated VEGF release, PDGF-BB release from Fn-P hydrogels was much slower than that from the native Fn hydrogels (Figure 3b). After demonstrating that the release of single growth factor can be controlled by the aptamers, we examined the release of both VEGF and PDGF-BB from dual aptamer-functionalized hydrogels. Similar results were acquired (Figure 3c). After 2 weeks, we also extracted the remaining growth factors from the Fn-B hydrogels. A total of 34.2% of PDGF-BB and 13.9% of VEGF were extracted, whereas nearly no growth factors could be extracted from the native Fn hydrogels (Figure 3c).

While we have shown that the two aptamers could control the release of VEGF and PDGF-BB from the Fn-Ap hydrogels, it is important to note that the kinetics of growth factor release can be adjusted by tuning the binding affinities of aptamers. Aptamers with different binding affinities can be either generated during the process of aptamer selection or developed through the change of their structures post-aptamer selection. For example, we have demonstrated the development of three subtypes of aptamers with different affinities via the mutation of the stem-loop structure.<sup>22</sup> Moreover, as aptamers have high binding specificities, in principle, more than two aptamers can be incorporated into the same hydrogel for controlling of the release of multiple growth factors with distinct release kinetics.

**3.3. Stimulation of Cells Using Released Growth Factors.** Growth factors usually have low stability and can easily lose their bioactivity during their storage or release from polymeric delivery systems. For instance, one study shows that VEGF bioactivity could decrease to  $\sim 15\%$  after 10 days of in vitro release from poly( $\epsilon$ -caprolactone-*co*-D,L-lactide) elastomers,<sup>47</sup> and another study shows that VEGF bioactivity could decrease to  $\sim 5\%$  after 1 week in vitro release from poly( $\epsilon$ -caprolactone)/collagen fibers.<sup>48</sup> Therefore, it is important to examine whether the growth factors in our Fn-Ap hydrogel systems were bioactive.

Before testing the bioactivity of released growth factors, we first examined how stock growth factors affect cells. We examined the survival, migration, and proliferation of endothelial cell (EC) and smooth muscle cell (SMC) treated with VEGF and PDGF-BB because it has been reported that

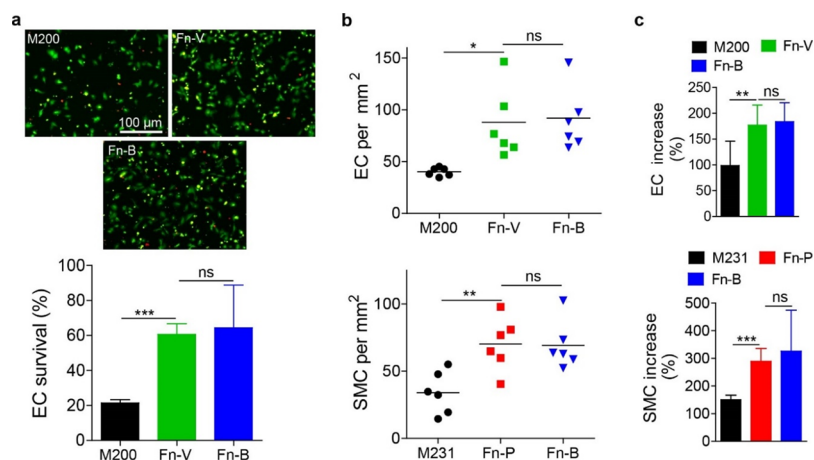


**Figure 4.** Examination of cell stimulation using the released growth factors. (a) EC survival after treatment with different release media for 48 h. M200, medium 200 supplemented with 1% FBS; Fn-V, VEGF released from ApV-functionalized Fn hydrogels; Fn-B, VEGF released from dual aptamer-functionalized Fn hydrogels. ECs were stained with the Live/Dead cell staining agents. (b, c) Cell migration (b) and proliferation (c). ECs were treated with medium 200 (M200) supplemented with 1% FBS or VEGF released from Fn-V or Fn-B. SMCs were treated with medium 231 (M231) supplemented with 1% FBS or PDGF-BB released from Fn-P or Fn-B.  $n = 6$ ; ns, no significant difference; \* $p < 0.05$ ; \*\* $p < 0.01$ ; \*\*\* $p < 0.001$ .

these growth factors can bind to cell receptors expressed by ECs and SMCs.<sup>49–51</sup> Both VEGF (10 ng/mL) alone and VEGF + PDGF-BB (10 ng/mL of VEGF and 10 ng/mL of PDGF-BB) enhanced the survival of ECs compared with PDGF-BB or the control medium without the supplemented growth factors (Figure S2a). SMCs had very high tolerance to low serum. Even after starvation for 2 days, most SMCs can still survive (Figure S2a). Our results also showed that stock VEGF and PDGF-BB could promote EC and SMC migration, respectively (Figure S2b), which is consistent with the literature.<sup>52,53</sup> We did not observe any synergistic effect or antagonistic effect of PDGF-BB and VEGF on either ECs or SMCs (Figure S2c). In addition, VEGF and PDGF-BB showed very high specificity in stimulating cell migration and proliferation.

We diluted the released growth factors from day 14 into 10 ng/mL and treated cells with the diluted growth factors. VEGF released from Fn-V could enhance the survival of ECs cultured in a low serum medium (Figure 4a and Figure S3). There was no significant difference between the release media collected from Fn-V and Fn-B. After showing that the released VEGF could enhance cell survival, we examined if the release growth factors could stimulate the migration (Figure 4b) and proliferation (Figure 4c) of ECs and SMCs. The data suggest that released VEGF and PDGF-BB could stimulate ECs and SMCs to migrate and proliferate, respectively.

**3.4. In Vitro Examination of Angiogenesis.** We further evaluated the effects of dual growth factors on angiogenesis using two types of in vitro angiogenesis assays. In the first assay, ECs were seeded on microbeads and embedded into different hydrogels. In the native Fn hydrogel that was loaded with VEGF and PDGF-BB (Fn + VP), few endothelial sprouts could be observed after 5 days (Figure 5a). This observation is reasonable since native Fn has low retention of growth factors and most of the loaded growth factors would be removed during the exchange of the cell culture media. In contrast, long tubular branches sprouting from the surface of the beads could be observed in the Fn-V hydrogels loaded with VEGF and in the Fn-B hydrogels loaded with both VEGF and PDGF-BB (Figure 5a). There was no significant difference in the number

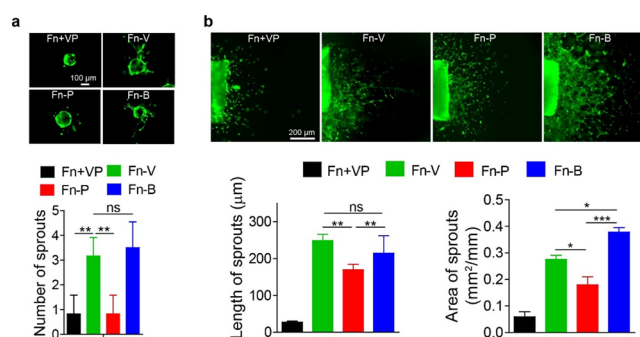


**Figure 5.** In vitro examination of angiogenesis. (a) Examination of endothelial cell (EC) sprouts from microbeads. Microbeads were coated with ECs and embedded into different hydrogels loaded with growth factors. Fn + VP, native Fn loaded with both VEGF and PDGF-BB. Fn-V, Fn-V loaded with VEGF; Fn-P, Fn-P loaded with PDGF-BB; Fn-B, Fn-B loaded with both VEGF and PDGF-BB. (b) Examination of aorta rings stimulated by different Fn hydrogels.  $n = 5$ ; ns, no significant difference; \* $p < 0.05$ ; \*\* $p < 0.01$ ; \*\*\* $p < 0.001$ .

of sprouts between Fn-V and Fn-B groups. This observation is consistent with the in vitro cell experiments showing that PDGF-BB did not affect ECs (Figure S2b,c and Figure 4). These data show that aptamer-mediated VEGF release can promote the growth of endothelial cells in the presence or absence of PDGF-BB.

To better mimic the in vivo angiogenesis, we cultured the aorta ring in the Fn-Ap hydrogel loaded with growth factors. This assay has been widely used to evaluate the angiogenic properties of growth factors.<sup>34,54</sup> Mouse aorta sections were seeded into collagen hydrogel, on top of which Fn hydrogels loaded with growth factors were placed. We did not directly embed the aorta rings in Fn hydrogels because VEGF-induced sprouting of micro-vessels is best observed in collagen hydrogels.<sup>34,54</sup> The data show that only a few scattered cells migrated in the Fn + VP group (Figure 5b). By contrast, long sprouting microvessel-like structures could be observed in other three groups including Fn-V loaded with VEGF, Fn-P loaded with PDGF-BB, and Fn-B loaded with VEGF + PDGF-BB (Figure 5b). Although there was no significant difference in

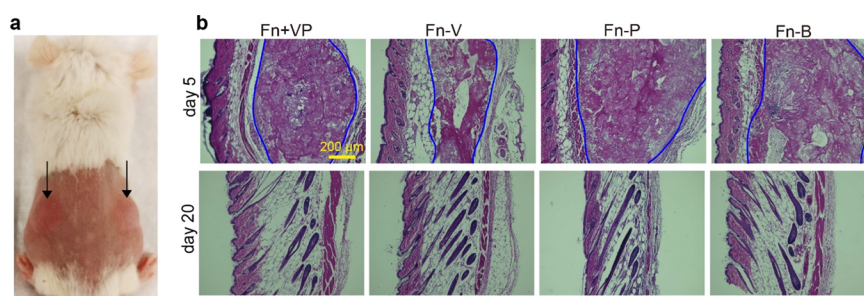


**Figure 6.** In situ injection of Fn-Ap hydrogels into mice. (a) Image of a mouse after in situ injection of hydrogels. Black arrows show the position of hydrogels. (b) H&E staining of Fn hydrogels and surrounding tissues at days 5 and 20 post-injection. Blue lines highlight the boundary between hydrogels and surrounding tissues.

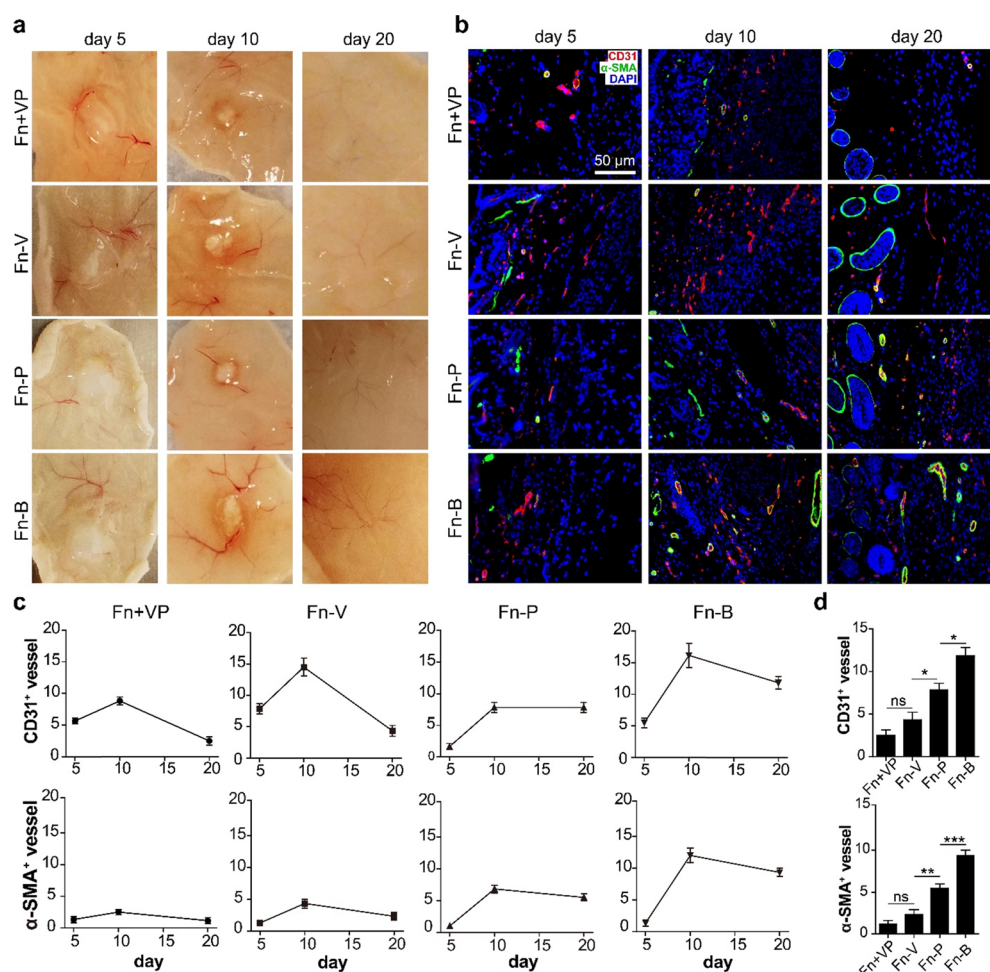


**Figure 7.** Examination of in vivo angiogenesis. (a) Representative macroscopic images of the skin tissues surrounding the Fn hydrogels. (b) Representative images of immunostaining of the skin tissues. (c) Quantification of CD31<sup>+</sup> and α-SMA<sup>+</sup> blood vessels per field. Error bars: standard errors. (d) Comparison of hydrogels in stimulating the growth of CD31<sup>+</sup> blood vessels (upper panel) and α-SMA<sup>+</sup> blood vessels (lower panel) at day 20.  $n = 4$ ; \* $p < 0.05$ ; \*\* $p < 0.01$ ; \*\*\* $p < 0.001$ .

the length of sprouting vessels between the Fn-V and Fn-B groups, the area of sprouts in the Fn-B group was significantly higher than those in the Fn-V and Fn-P groups. The results also suggest that cells form a dense network structure in the Fn-B group (Figure 5b).

ECs and SMCs are the major cell types in the native aorta. When both VEGF and PDGF-BB were present around the aorta, each growth factor could stimulate its own target cells for migration and proliferation. Combining the effect of VEGF on ECs and PDGF-BB on SMCs, it is reasonable that the aorta

rings in the Fn-B group had a significantly higher area of sprouts compared with other groups. Taken together, the results of in vitro angiogenesis suggest that aptamer-mediated codelivery of dual growth factors would lead to a better outcome of angiogenesis.

**3.5. In Vivo Examination of Angiogenesis.** After acquiring the promising in vitro results, we evaluated whether controlled release of dual growth factors from the Fn-B hydrogel could promote the formation of mature blood vessels in vivo. A large bump was observed after the in situ injection of

the reaction mixture (Figure 6a), suggesting the formation of the hydrogels. It is confirmed by H&E staining that all the injected hydrogels were in the hypodermal layer of the skin at least during the first 5 days post-injection (Figure 6b). The hydrogels disappeared in the injection sites at day 20 post-injection (Figure 6b). It suggests that in situ injectable aptamer-functionalized Fn hydrogels are biodegradable.

Consistent with the results shown in Figure 6b, macroscopic images show that Fn hydrogels could be observed within the first 10 days but completely degraded by day 20 (Figure 7a). Blood vessels could be observed in the tissues surrounding Fn hydrogels in all four groups during the first 10 days. In addition to the macroscopic observation, we stained the skin tissues with anti-CD31 antibody and anti- $\alpha$ -SMA antibody and quantified the number of blood vessels (Figure 7b–d). We used these two antibodies for tissue staining since CD31 is a typical endothelial marker and  $\alpha$ -SMA is a typical mural cell marker of mature blood vessels.<sup>55,56</sup> Notably, skin appendages (hair follicles and sebaceous glands) exhibit autofluorescence (Figure S4c). They were excluded from the quantification of blood vessels based on their morphology and patterns.

In all four groups, the number of CD31<sup>+</sup> vessels increased from day 5 to day 10 (Figure 7c). The number of CD31<sup>+</sup> vessels in the Fn + VP and Fn-V groups sharply decreased from day 10 to day 20 (Figure 7c). The number of CD31<sup>+</sup> vessels slightly decreased in the Fn-B group and barely changed in the Fn-P group from day 10 to day 20 (Figure 7c). The number of  $\alpha$ -SMA<sup>+</sup> vessels was much fewer than that of CD31<sup>+</sup> vessels throughout the entire study in both Fn + VP and Fn-V groups. The number of  $\alpha$ -SMA<sup>+</sup> vessels was comparable to that of CD31<sup>+</sup> vessels in both Fn-P and Fn-B groups. Notably, the Fn-B group showed the highest CD31<sup>+</sup> and  $\alpha$ -SMA<sup>+</sup> vessels at day 20 among all four groups (Figure 7d), and numerous blood vessels consisted of CD31<sup>+</sup> endothelial cells covered by a layer of  $\alpha$ -SMA<sup>+</sup> mural cells (Figure 7b). These results suggest that VEGF delivery could quickly stimulate the proliferation of endothelial cells for the growth of blood vessels and, more importantly, that aptamer-mediated codelivery of VEGF and PDGF-BB could promote the formation of mature and stable blood vessels. However, it is important to note that the current hydrogel is a sequential VEGF and PDGF-BB release system with faster VEGF and slower PDGF-BB release kinetics. It is possible to further tune their release kinetics by changing the binding affinities and densities of the aptamers and examine how the different combinations of release kinetics affect angiogenesis in the future work.

VEGF and PDGF-BB have been previously studied for angiogenesis. However, opposite results were acquired. Greenberg et al. found that PDGF-BB could stimulate angiogenesis but VEGF inhibited PDGF-BB-mediated angiogenesis through VEGF-R2.<sup>57</sup> Our results show that PDGF-BB alone indeed promoted angiogenesis, but the codelivery of VEGF and PDGF-BB further enhanced angiogenesis. While the exact reason for this discrepancy is unclear, one possibility is that the delivery systems used in different studies are different. Greenberg et al. used Matrigel in their study, whereas Matrigel releases growth factors very quickly.<sup>58</sup> This possibility highlights the necessity of advancing polymer systems for optimal delivery of angiogenic factors.

Different polymer systems were studied for the delivery of angiogenic factors, including poly(lactide-co-glycolide) systems,<sup>59</sup> Fn hydrogels loaded with heparin coacervates,<sup>60</sup> Fn hydrogels loaded with peptide-functionalized growth factors,<sup>46</sup>

etc. Compared with these polymer systems for controlled release of angiogenic factors, one major advantage of the Fn-Ap system is that aptamers have high binding affinities and specificities. The density of aptamers in the hydrogels can be facilely changed depending on the need. Thus, the release kinetics can be tuned by changing the binding affinity and incorporation density of aptamers. Moreover, in our system, angiogenic factors do not need to be chemically or biologically functionalized with any moieties. It would ensure the maintenance of their bioactivity and involve fewer regulation issues for future applications.

## 4. CONCLUSIONS

This work has demonstrated that aptamer-functionalized Fg can be used to develop in situ injectable dual aptamer-functionalized Fn hydrogels under physiological conditions. Through the aptamer functionalization, Fn hydrogels can stably sequester VEGF and PDGF-BB, controlling their release in a sustained and sequential manner. The released VEGF and PDGF-BB can maintain high bioactivity to stimulate the growth of corresponding endothelial cells and smooth muscle cells. Importantly, codelivery of VEGF and PDGF-BB using the dual aptamer-functionalized in situ injectable Fn hydrogels can significantly promote the formation of mature blood vessel. Therefore, we envision that this dual aptamer-functionalized in situ injectable hydrogel system holds great potential for biomedical applications such as drug delivery and regenerative medicine.

## ■ ASSOCIATED CONTENT

### 📄 Supporting Information

The Supporting Information is available free of charge on the ACS Publications website at DOI: 10.1021/acsami.9b02462.

Characterization of Fn-V and Fn-P hydrogels, effect of stock growth factors on endothelial cells and smooth muscle cells, MTS assay of endothelial cell survival, staining of CD31 and  $\alpha$ -SMA, DNA sequences, and aptamer conjugation efficiency (PDF)

## ■ AUTHOR INFORMATION

### Corresponding Author

\*E-mail: yxw30@psu.edu. Phone: 814-865-6867.

### ORCID

Yong Wang: 0000-0002-2244-1742

### Notes

The authors declare no competing financial interest.

## ■ ACKNOWLEDGMENTS

The authors thank Huck Institutes of the Life Sciences and Material Characterization Lab at Pennsylvania State University (University Park, PA) for technical training and support. This study was, in part, supported by the National Institutes of Health (HL122311 and AR073364).

## ■ REFERENCES

- (1) Seliktar, D. Designing Cell-Compatible Hydrogels for Biomedical Applications. *Science* **2012**, *336*, 1124–1128.
- (2) Slaughter, B. V.; Khurshid, S. S.; Fisher, O. Z.; Khademhosseini, A.; Peppas, N. A. Hydrogels in Regenerative Medicine. *Adv. Mater.* **2009**, *21*, 3307–3329.
- (3) Hoare, T. R.; Kohane, D. S. Hydrogels in Drug Delivery: Progress and Challenges. *Polymer* **2008**, *49*, 1993–2007.

- (4) Peattie, R. A.; Nayate, A. P.; Firpo, M. A.; Shelby, J.; Fisher, R. J.; Prestwich, G. D. Stimulation of in Vivo Angiogenesis by Cytokine-Loaded Hyaluronic Acid Hydrogel Implants. *Biomaterials* **2004**, *25*, 2789–2798.
- (5) Yu, L.; Ding, J. Injectable Hydrogels as Unique Biomedical Materials. *Chem. Soc. Rev.* **2008**, *37*, 1473–1481.
- (6) Tan, H.; Chu, C. R.; Payne, K. A.; Marra, K. G. Injectable in Situ Forming Biodegradable Chitosan–Hyaluronic Acid Based Hydrogels for Cartilage Tissue Engineering. *Biomaterials* **2009**, *30*, 2499–2506.
- (7) Yang, J.-A.; Yeom, J.; Hwang, B. W.; Hoffman, A. S.; Hahn, S. K. In Situ-Forming Injectable Hydrogels for Regenerative Medicine. *Prog. Polym. Sci.* **2014**, *39*, 1973–1986.
- (8) Shu, X. Z.; Liu, Y.; Palumbo, F. S.; Luo, Y.; Prestwich, G. D. In Situ Crosslinkable Hyaluronan Hydrogels for Tissue Engineering. *Biomaterials* **2004**, *25*, 1339–1348.
- (9) Ruel-Gariépy, E.; Leroux, J.-C. In Situ-Forming Hydrogels—Review of Temperature-Sensitive Systems. *Eur. J. Pharm. Biopharm.* **2004**, *58*, 409–426.
- (10) Huynh, D. P.; Im, G. J.; Chae, S. Y.; Lee, K. C.; Lee, D. S. Controlled Release of Insulin from pH/Temperature-Sensitive Injectable Pentablock Copolymer Hydrogel. *J. Controlled Release* **2009**, *137*, 20–24.
- (11) Suzuki, A.; Tanaka, T. Phase Transition in Polymer Gels Induced by Visible Light. *Nature* **1990**, *346*, 345–347.
- (12) He, C.; Kim, S. W.; Lee, D. S. In Situ Gelling Stimuli-Sensitive Block Copolymer Hydrogels for Drug Delivery. *J. Controlled Release* **2008**, *127*, 189–207.
- (13) Rowley, J. A.; Madlambayan, G.; Mooney, D. J. Alginate Hydrogels as Synthetic Extracellular Matrix Materials. *Biomaterials* **1999**, *20*, 45–53.
- (14) Ahmed, T. A. E.; Dare, E. V.; Hincke, M. Fibrin: A Versatile Scaffold for Tissue Engineering Applications. *Tissue Eng., Part B* **2008**, *14*, 199–215.
- (15) Zhang, X.-Z.; Lewis, P. J.; Chu, C.-C. Fabrication and Characterization of a Smart Drug Delivery System: Microsphere in Hydrogel. *Biomaterials* **2005**, *26*, 3299–3309.
- (16) Ellington, A. D.; Szostak, J. W. In Vitro Selection of RNA Molecules That Bind Specific Ligands. *Nature* **1990**, *346*, 818–822.
- (17) Keefe, A. D.; Pai, S.; Ellington, A. Aptamers as Therapeutics. *Nat. Rev. Drug Discovery* **2010**, *9*, 537–550.
- (18) Ng, E. W. M.; Shima, D. T.; Calias, P.; Cunningham, E. T., Jr.; Guyer, D. R.; Adamis, A. P. Pegaptanib, a Targeted Anti-VEGF Aptamer for Ocular Vascular Disease. *Nat. Rev. Drug Discovery* **2006**, *5*, 123–132.
- (19) Zhao, N.; Battig, M. R.; Xu, M.; Wang, X.; Xiong, N.; Wang, Y. Development of a Dual-Functional Hydrogel Using RGD and Anti-VEGF Aptamer. *Macromol. Biosci.* **2017**, *17*, 1700201.
- (20) Lai, J.; Jiang, P.; Gaddes, E. R.; Zhao, N.; Abune, L.; Wang, Y. Aptamer-Functionalized Hydrogel for Self-Programmed Protein Release via Sequential Photoreaction and Hybridization. *Chem. Mater.* **2017**, *29*, 5850–5857.
- (21) Zhang, X.; Battig, M. R.; Chen, N.; Gaddes, E. R.; Duncan, K. L.; Wang, Y. Chimeric Aptamer-Gelatin Hydrogels as an Extracellular Matrix Mimic for Loading Cells and Growth Factors. *Biomacromolecules* **2016**, *17*, 778–787.
- (22) Battig, M. R.; Huang, Y.; Chen, N.; Wang, Y. Aptamer-Functionalized Superporous Hydrogels for Sequestration and Release of Growth Factors Regulated via Molecular Recognition. *Biomaterials* **2014**, *35*, 8040–8048.
- (23) Soontornworajit, B.; Zhou, J.; Zhang, Z.; Wang, Y. Aptamer-Functionalized in Situ Injectable Hydrogel for Controlled Protein Release. *Biomacromolecules* **2010**, *11*, 2724–2730.
- (24) Battig, M. R.; Soontornworajit, B.; Wang, Y. Programmable Release of Multiple Protein Drugs from Aptamer-Functionalized Hydrogels via Nucleic Acid Hybridization. *J. Am. Chem. Soc.* **2012**, *134*, 12410–12413.
- (25) Soontornworajit, B.; Zhou, J.; Snipes, M. P.; Battig, M. R.; Wang, Y. Affinity Hydrogels for Controlled Protein Release Using Nucleic Acid Aptamers and Complementary Oligonucleotides. *Biomaterials* **2011**, *32*, 6839–6849.
- (26) Stejskalová, A.; Oliva, N.; England, F. J.; Almquist, B. D. Biologically Inspired, Cell-Selective Release of Aptamer-Trapped Growth Factors by Traction Forces. *Adv. Mater.* **2019**, 1806380.
- (27) Zhang, Z.; Han, J.; Pei, Y.; Fan, R.; Du, J. Chaperone Copolymer-Assisted Aptamer-Patterned DNA Hydrogels for Triggering Spatiotemporal Release of Protein. *ACS Appl. Bio Mater.* **2018**, *1*, 1206–1214.
- (28) Liu, C.; Han, J.; Pei, Y.; Du, J. Aptamer Functionalized DNA Hydrogel for Wise-Stage Controlled Protein Release. *Appl. Sci.* **2018**, *8*, 1941.
- (29) Barsotti, M. C.; Felice, F.; Balbarini, A.; Di Stefano, R. Fibrin as a Scaffold for Cardiac Tissue Engineering. *Biotechnol. Appl. Biochem.* **2011**, *58*, 301–310.
- (30) Janmey, P. A.; Winer, J. P.; Weisel, J. W. Fibrin Gels and Their Clinical and Bioengineering Applications. *J. R. Soc., Interface* **2008**, *6*, 1–10.
- (31) Mosesson, M. W. Fibrinogen and Fibrin Structure and Functions. *J. Thromb. Haemostasis* **2005**, *3*, 1894–1904.
- (32) Zhao, N.; Coyne, J.; Xu, M.; Zhang, X.; Suzuki, A.; Shi, P.; Lai, J.; Fong, G.-H.; Xiong, N.; Wang, Y. Assembly of Bifunctional Aptamer-Fibrinogen Macromer for VEGF Delivery and Skin Wound Healing. *Chem. Mater.* **2019**, 1006–1015.
- (33) Soon, A. S. C.; Lee, C. S.; Barker, T. H. Modulation of Fibrin Matrix Properties via Knob: Hole Affinity Interactions Using Peptide–PEG Conjugates. *Biomaterials* **2011**, *32*, 4406–4414.
- (34) Baker, M.; Robinson, S. D.; Lechertier, T.; Barber, P. R.; Tavora, B.; D'amico, G.; Jones, D. T.; Vojnovic, B.; Hodivala-Dilke, K. Use of the Mouse Aortic Ring Assay to Study Angiogenesis. *Nat. Protoc.* **2012**, *7*, 89–104.
- (35) Drury, J. L.; Mooney, D. J. Hydrogels for Tissue Engineering: Scaffold Design Variables and Applications. *Biomaterials* **2003**, *24*, 4337–4351.
- (36) Annabi, N.; Nichol, J. W.; Zhong, X.; Ji, C.; Koshy, S.; Khademhosseini, A.; Dehghani, F. Controlling the Porosity and Microarchitecture of Hydrogels for Tissue Engineering. *Tissue Eng., Part B* **2010**, *16*, 371–383.
- (37) Geckil, H.; Xu, F.; Zhang, X.; Moon, S.; Demirci, U. Engineering Hydrogels as Extracellular Matrix Mimics. *Nanomedicine* **2010**, *5*, 469–484.
- (38) Zisch, A. H.; Lutolf, M. P.; Hubbell, J. A. Biopolymeric Delivery Matrices for Angiogenic Growth Factors. *Cardiovasc. Pathol.* **2003**, *12*, 295–310.
- (39) Johnson, K. E.; Wilgus, T. A. Vascular Endothelial Growth Factor and Angiogenesis in the Regulation of Cutaneous Wound Repair. *Adv. Wound Care* **2014**, *3*, 647–661.
- (40) Carmeliet, P.; Jain, R. K. Molecular Mechanisms and Clinical Applications of Angiogenesis. *Nature* **2011**, *473*, 298–307.
- (41) Brudno, Y.; Ennett-Shepard, A. B.; Chen, R. R.; Aizenberg, M.; Mooney, D. J. Enhancing Microvascular Formation and Vessel Maturation through Temporal Control over Multiple Pro-Angiogenic and Pro-Maturation Factors. *Biomaterials* **2013**, *34*, 9201–9209.
- (42) Golub, J. S.; Kim, Y.-t.; Duvall, C. L.; Bellamkonda, R. V.; Gupta, D.; Lin, A. S.; Weiss, D.; Taylor, W. R.; Guldberg, R. E. Sustained VEGF Delivery via PLGA Nanoparticles Promotes Vascular Growth. *Am. J. Physiol.: Heart Circ. Physiol.* **2010**, *298*, 1959–1965.
- (43) Sacchi, V.; Mittermayr, R.; Hartinger, J.; Martino, M. M.; Lorentz, K. M.; Wolbank, S.; Hofmann, A.; Largo, R. A.; Marschall, J. S.; Groppa, E.; Gianni-Barrera, R.; Ehrbar, M.; Hubbell, J. A.; Redl, H.; Banfi, A. Long-Lasting Fibrin Matrices Ensure Stable and Functional Angiogenesis by Highly Tunable, Sustained Delivery of Recombinant VEGF164. *Proc. Natl. Acad. Sci.* **2014**, *111*, 6952–6957.
- (44) Yancopoulos, G. D.; Davis, S.; Gale, N. W.; Rudge, J. S.; Wiegand, S. J.; Holash, J. Vascular-Specific Growth Factors and Blood Vessel Formation. *Nature* **2000**, *407*, 242–248.
- (45) Almany, L.; Seliktar, D. Biosynthetic Hydrogel Scaffolds Made from Fibrinogen and Polyethylene Glycol for 3D Cell Cultures. *Biomaterials* **2005**, *26*, 2467–2477.

(46) Martino, M. M.; Briquez, P. S.; Güç, E.; Tortelli, F.; Kilarski, W. W.; Metzger, S.; Rice, J. J.; Kuhn, G. A.; Müller, R.; Swartz, M. A.; Hubbell, J. A. Growth Factors Engineered for Super-Affinity to the Extracellular Matrix Enhance Tissue Healing. *Science* **2014**, *343*, 885–888.

(47) Gu, F.; Neufeld, R.; Amsden, B. Sustained Release of Bioactive Therapeutic Proteins from a Biodegradable Elastomeric Device. *J. Controlled Release* **2007**, *117*, 80–89.

(48) Ekaputra, A. K.; Prestwich, G. D.; Cool, S. M.; Hutmacher, D. W. The Three-Dimensional Vascularization of Growth Factor-Releasing Hybrid Scaffold of Poly (*ε*-Caprolactone)/Collagen Fibers and Hyaluronic Acid Hydrogel. *Biomaterials* **2011**, *32*, 8108–8117.

(49) Gerber, H.-P.; McMurtrey, A.; Kowalski, J.; Yan, M.; Keyt, B. A.; Dixit, V.; Ferrara, N. Vascular Endothelial Growth Factor Regulates Endothelial Cell Survival through the Phosphatidylinositol 3'-Kinase/Akt Signal Transduction Pathway Requirement for Flk-1/Kdr Activation. *J. Biol. Chem.* **1998**, *273*, 30336–30343.

(50) Rodrigues, M.; Griffith, L. G.; Wells, A. Growth Factor Regulation of Proliferation and Survival of Multipotential Stromal Cells. *Stem Cell Res. Ther.* **2010**, *1*, 32–44.

(51) Sondell, M.; Lundborg, G.; Kanje, M. Vascular Endothelial Growth Factor Has Neurotrophic Activity and Stimulates Axonal Outgrowth, Enhancing Cell Survival and Schwann Cell Proliferation in the Peripheral Nervous System. *J. Neurosci.* **1999**, *19*, 5731–5740.

(52) Dimmeler, S.; Dernbach, E.; Zeiher, A. M. Phosphorylation of the Endothelial Nitric Oxide Synthase at Ser-1177 Is Required for VEGF-Induced Endothelial Cell Migration. *FEBS Lett.* **2000**, *477*, 258–262.

(53) Jawien, A.; Bowen-Pope, D. F.; Lindner, V.; Schwartz, S. M.; Clowes, A. W. Platelet-Derived Growth Factor Promotes Smooth Muscle Migration and Intimal Thickening in a Rat Model of Balloon Angioplasty. *J. Clin. Invest.* **1992**, *89*, 507–511.

(54) Zippel, N.; Ding, Y.; Fleming, I. A Modified Aortic Ring Assay to Assess Angiogenic Potential in Vitro. In *Angiogenesis Protocols*; Springer; 2016; pp 205–219.

(55) Miettinen, M.; Lindenmayer, A. E.; Chaubal, A. Endothelial Cell Markers Cd31, Cd34, and Bnh9 Antibody to H-and Y-Antigens—Evaluation of Their Specificity and Sensitivity in the Diagnosis of Vascular Tumors and Comparison with Von Willebrand Factor. *Mod. Pathol.* **1994**, *7*, 82–90.

(56) Lebrin, F.; Srun, S.; Raymond, K.; Martin, S.; van den Brink, S.; Freitas, C.; Bréant, C.; Mathivet, T.; Larrivé, B.; Thomas, J.-L.; Arthur, H. M.; Westermann, C. J. J.; Disch, F.; Mager, J. J.; Snijder, R. J.; Eichmann, A.; Mummery, C. L. Thalidomide Stimulates Vessel Maturation and Reduces Epistaxis in Individuals with Hereditary Hemorrhagic Telangiectasia. *Nat. Med.* **2010**, *16*, 420–428.

(57) Greenberg, J. L.; Shields, D. J.; Barillas, S. G.; Acevedo, L. M.; Murphy, E.; Huang, J.; Schepke, L.; Stockmann, C.; Johnson, R. S.; Angle, N.; Cheresch, D. A. A Role for VEGF as a Negative Regulator of Pericyte Function and Vessel Maturation. *Nature* **2008**, *456*, 809–813.

(58) Poldervaart, M. T.; Gremmels, H.; van Deventer, K.; Fledderus, J. O.; Öner, F. C.; Verhaar, M. C.; Dhert, W. J. A.; Alblas, J. Prolonged Presence of VEGF Promotes Vascularization in 3D Bioprinted Scaffolds with Defined Architecture. *J. Controlled Release* **2014**, *184*, 58–66.

(59) Richardson, T. P.; Peters, M. C.; Ennett, A. B.; Mooney, D. J. Polymeric System for Dual Growth Factor Delivery. *Nat. Biotechnol.* **2001**, *19*, 1029–1034.

(60) Awada, H. K.; Johnson, N. R.; Wang, Y. Sequential Delivery of Angiogenic Growth Factors Improves Revascularization and Heart Function after Myocardial Infarction. *J. Controlled Release* **2015**, *207*, 7–17.